

Renormalized linked-cluster expansion for strongly correlated lattice fermions in $d = \infty$ dimensions

M. Bartkowiak* and K. A. Chao

Division of Physics, Department of Physics and Mathematics, The University of Trondheim, Norwegian Institute of Technology, N-7034 Trondheim, Norway

(Received 17 July 1992)

We show that mean-field-type symmetry-breaking approximations for correlated fermions can be constructed by performing vertex renormalization (VR) in the linked-cluster expansion, just as for the case of lattice spin models. In the limit of infinite spatial dimensions we sum up exactly the renormalized diagrams for the grand-canonical potential of the Hubbard model and, using the diagrammatic technique for Hubbard operators, we construct explicitly an approximate VR. The procedure leads to a self-consistent symmetry breaking analogous to that of the mean-field theory for spin systems. We present solutions for the case of half-filled energy band. They are valid for arbitrary temperatures and become exact for both large- U limit and for $U = 0$. The antiferromagnetic order parameter is found to have the conventional mean-field form and, in the regime of strong correlations, the obtained critical temperature coincides with the mean-field-theory result for the Néel temperature of the effective Heisenberg Hamiltonian.

I. INTRODUCTION

Just like the Heisenberg model in the theory of spin systems, the Hubbard model¹ has become a standard model for correlated fermions on a lattice. However, in contrast to the former, properties of the latter are still far from being well understood. Exact results exist only in a few special cases, such as in one spatial dimension, and provide very little information about the general one, so that even qualitative structure of the corresponding phase diagram is still disputed. The Hubbard model has been studied with the aid of many approximation schemes, but the results are often conflicting. Therefore, it is essential to establish a general unifying approach to construct systematic approximations valid for the whole range of the Hamiltonian parameters and for arbitrary temperatures. As a general guideline, one can follow the techniques and approximation schemes which had proved successful in the theory of spin systems such as the Ising or Heisenberg model. Just like the localized noninteracting spins in the case of the latter, the system of uncoupled lattice sites for the case of strongly correlated fermions (e.g., atomic limit of the Hubbard model) should be taken as the starting point. We will follow this analogy and show it to be very fruitful.

The simplest theory of the localized spin systems is certainly the mean-field theory (MFT). Although it is based on a gross simplification of the underlying physics, it often provides a good qualitative description of a spin system. Moreover, it is well established that the MFT of classical and quantum spin lattice models gives the exact description of their properties for a high coordination number of the lattice z , i.e., for spatial dimension $d \rightarrow \infty$. The situation is fundamentally different in the case of fermionic lattice models, i.e., models with itinerant quantum-mechanical degrees of freedom. Here, usu-

ally the Hartree-Fock approximation (HFA) is regarded as a mean-field theory. However, within this approximation, fluctuations in the intrasite interaction are neglected, although for the case of strong correlation they never become small, independent of spatial dimension. Therefore, unlike the mean-field approximation (MFA) for spin systems, the HFA for lattice fermions with short-range interaction *does not* become exact in the limit $d \rightarrow \infty$.²⁻⁴

On the other hand, the concept of high dimensions was introduced three years ago² as a new approach to correlated Fermi systems on a lattice. It has been shown that fermion systems with proper scaling of the hopping rate in the kinetic energy become much simpler in high dimensions, but keep away from getting trivial. Since then, the study of high-dimensional Fermi systems has been very fruitful^{3,5} and has led, e.g., to the exact $d = \infty$ solutions of the Falicov-Kimball model.⁶ However, the most interesting problem, the exact solution of the Hubbard model in this limit, remains unsolved, although the recent Monte Carlo study by Jarrell⁷ provides very useful information.

The fact that the proper self-energy of a system of interacting fermions becomes site diagonal in high dimension^{2,3} implies that it is sufficient to solve an *atomic* problem in a generalized time-dependent effective field. The situation is thus similar to the MFT for spin systems, where the effective field is the Weiss field. This analogy has been recently used to study the Falicov-Kimball model on a Bethe lattice.⁴ It has been shown that it is possible in this case to construct a mean-field-type Hamiltonian where the "mean fields" are fermion operators. In analogy to the MFT for spin systems, it is then intuitively clear that when the coordination number of the Bethe lattice $z \rightarrow \infty$, the mean-field Hamiltonian becomes exact. Indeed, the corresponding results

are qualitatively similar to those for the $d = \infty$ hypercubic lattice.⁶ However, if we are to construct a general MFT for fermionic lattice models and show rigorously that it becomes exact in high dimension, we need a more solid basis.

For systems of localized spins, one of the most successful tools to study critical phenomena and to construct useful self-consistent approximations is the expansion of thermodynamic quantities as power series of intersite coupling constants.⁸ One then naturally expects that similar perturbation expansion around the atomic limit should yield the required basis to develop MFT for correlated fermions which, moreover, can be systematically improved. Recently Metzner⁹ derived systematically the linked-cluster expansion (LCE) for the Hubbard model in analogy to that known for the Ising model.¹⁰ In this approach only *connected diagrams* and *unrestricted lattice sums* (the so-called “free embedding”) are involved, due to the use of the cumulant representation. This, in principle, allows one to perform vertex renormalization (VR) and, following the analogy with the Ising model, construct self-consistent approximations.

In fact, the expansion in powers of intersite coupling constants is not new in the theory of correlated fermions. For the Hubbard model, several static quantities such as the grand-canonical potential and some static susceptibilities have been expanded in powers of the hopping parameter t up to the fourth,^{11,12} the sixth,¹³ and recently to the eighth and ninth¹⁴ order using different techniques, including the LCE.^{12,13} For fixed values of the Hamiltonian parameters, the above expansions become the high-temperature series expansions. This is again analogical to the theory of spin systems, where the LCE in powers of the exchange integral can be used to generate high-temperature series.¹⁵

Anyhow, it is only the LCE which is suitable for renormalization, and just the VR is the fundamental concept for construction of self-consistent approximations. Let us recall our analogy with the theory of spin systems to clarify the problem. In the LCE for the Ising model,¹⁰ the VR in the lowest order of the diagrammatic expansion for free energy reproduces the MFT results. Simultaneously, the class of diagrams which is summed up in this renormalization procedure consists of all loopless diagrams (Cayley trees), i.e., diagrams which do not depend on the structure and coordination number z of the lattice or, in other words, diagrams which carry factor $(1/z)^0$. All other diagrams are at least of order $1/z$, provided that the exchange parameter is properly scaled to keep the Ising model nontrivial when $z \rightarrow \infty$. The required scaling is simply $J = J^*/z$ with fixed J^* . Therefore, the LCE in this case provides a formal basis to show that the MFT becomes exact in infinite dimension. Moreover, it is then easy to classify diagrams by powers of $1/z$, and generate $1/z$ (or $1/d$) expansion for hypercubic lattices in a way similar to that recently proposed by Fishman and Vignale.¹⁶ The problem which we address in this paper is to show how the above scenario can in practice be generalized to the case of strongly correlated fermions.

A general analysis of z dependence of the LCE diagrams for the Hubbard model with the scaling of the hop-

ping parameter $t = t^*/\sqrt{z}$ (t^* fixed), required to obtain a nontrivial infinite dimensional limit, has been done by Metzner.⁹ However, his diagrammatic technique is very difficult to use in practical calculation. Difficulties arise even at the level of unrenormalized expansion and reduce to the problem of calculation of atomic cumulants represented diagrammatically by vertices. Since the standard Wick theorem for fermion operators cannot be applied, Metzner has proposed a method based on calculation of functional derivatives of a generating functional with respect to auxiliary Grassmann fields. This, however, is very inconvenient for practical purposes. Therefore, we shall again refer the analogy with the theory of spin systems to find a better approach.

The above mentioned difficulties are related to the quantum nature of the considered system, and are very similar to those which appear in the LCE for quantum spin systems like the Heisenberg model. There, since commutators of two spin operators are not c numbers, but other spin operators, calculation of \mathcal{T} -ordered products becomes very difficult. On the other hand, the commutators are *linear* in spin operators. This is, in fact, sufficient to prove a *generalized Wick theorem*,¹⁷ and simplify the problem considerably. Based on such a generalized Wick theorem, a diagrammatic technique for spin operators has been constructed and successfully used to study the Heisenberg model¹⁸ (for details and further references see Ref. 19).

Adaptation of this concept to the LCE for strongly correlated fermions requires further generalizations. The first attempt was due to Hubbard, who introduced convenient single-site operators (which also had linear commutation relations), usually referred to as Hubbard operators (HO).²⁰ His initiative became fully developed when a generalized Wick theorem for HO was proved and diagrammatic techniques constructed^{21–23} (see also Ref. 19). In comparison with the standard diagrammatic technique for fermion operators, diagrams for the HO have a somewhat peculiar form. Application of the generalized Wick theorem implies appearance of *both fermion and boson* Green’s-function lines, as well as vertices at which *several* such lines merge to create another one. Moreover, since within the LCE, \mathcal{T} -ordered products of HO are expressed in terms of cumulants, they are represented diagrammatically by so-called “single-site blocks,”^{22,23} sums of which correspond to bare vertices in the diagrammatic technique of Metzner.⁹ His technique is thus basically the same as that for HO, but within the framework of the latter vertices gain inner structure and become single-site blocks, so that *it is possible to evaluate atomic cumulants diagrammatically*. Consequently, it is much more useful for practical purposes (particularly in selective summations of classes of diagrams) and we will use it in this paper.

The concept of VR in the LCE is related to the problem of symmetry breaking. It is impossible to obtain symmetry-broken solutions in any finite order of the unrenormalized LCE, which is the situation analogical to that in high-temperature series expansions. Therefore, in order to be able to study ordered phases, one has to sum up certain infinite classes of diagrams. For the case

of the spin systems, the simplest symmetry-breaking approximation is the MFA, and the corresponding class of diagrams summed up is the class of Cayley trees. This summation, on the other hand, is done by performing the VR. It is thus reasonable to expect that the vertex-renormalized LCE provides a basis to construct self-consistent symmetry-breaking approximations in general.

VR in the LCE for the Ising model had been introduced many years ago^{24,25} (for a review, see Ref. 10), but in practice only two self-consistent Φ -derivable approximations beyond MFA, and only for the Ising model, have been systematically studied and used: the renormalized second order of the LCE,²⁶ and the renormalized single-loop approximation.^{24,27,28} Actually, only the former leads to an acceptable description of the thermodynamic properties of the Ising model in the whole range of temperatures, whereas the latter fails in the critical region, leading to a discontinuous phase transition^{26,28} (this fact is related to the lack of a small parameter in the loop-expansion theory for spin systems^{16,29}). Although a systematic generalization of the vertex renormalized LCE to the case of the Hubbard model has been introduced only recently,⁹ some concepts of the VR can be found in previous works concerning electron correlations.^{19,28,30}

Anyhow, no systematic renormalizations have been done for fermionic lattice models until recently, when we managed to perform explicitly an approximate VR in the simplest, second order of the LCE for the Hubbard model.³¹ We have shown that, as expected, also for this case, an approach based on the VR leads to a self-consistent symmetry breaking and that the resulting approximation scheme is valid for the whole range of temperatures in the region of strong correlations. Moreover, character of the obtained self-consistent equations and corresponding solutions are very similar to those in the MFA for spin systems. Finally, it has been shown that the obtained results are exact to the second order in t/U in the limit of infinite dimension, and that the proposed approach gives a crossover from large- U Heisenberg mean-field behavior to zero Néel temperature at $U = 0$. In this paper we extend our previous consideration to the case of the class of diagrams which become exact when $d \rightarrow \infty$.

This paper is structured as follows. In Sec. II we briefly describe how the LCE for the Hubbard model is constructed and introduce the concept of VR.^{9,10} Derivation of the exact diagrammatic expression for the thermodynamic potential for the case of infinite lattice dimension is presented in Sec. III. In Sec. IV we introduce the diagrammatic technique for HO and use it to perform an approximate VR. The results for the case of the half-filled energy band are presented in Sec. V, and conclusions in Sec. VI close the presentation.

II. LINKED-CLUSTER EXPANSION FOR THE HUBBARD MODEL

We consider a system of N sites on a d -dimensional hypercubic lattice with n electrons per site in an external magnetic field $h_i = h \pm h_s$ consisting of a uniform field h and a staggered one h_s . In conventional notation we write the single-band grand-canonical Hubbard Hamiltonian as

$$H = H_0 + H_1, \quad (1)$$

where

$$H_0 = U \sum_i n_{i+} n_{i-} - \sum_i \sum_{\sigma} (\mu + \sigma h_i) n_{i\sigma} \quad (2)$$

is the atomic limit of the Hubbard model, and

$$H_1 = \sum_{ij} \sum_{\sigma} t_{ij} c_{i\sigma}^{\dagger} c_{j\sigma} \quad (3)$$

will be treated as a perturbation. The intersite hopping transitions are restricted only to nearest neighbors,

$$t_{ij} = \begin{cases} -t & \text{when } i \text{ and } j \text{ are nearest neighbors} \\ 0 & \text{otherwise.} \end{cases} \quad (4)$$

The grand-canonical potential,

$$\Omega = -\frac{1}{\beta} \ln \text{Tr} \exp(-\beta H), \quad (5)$$

can be expressed in terms of the averages with respect to the unperturbed Hamiltonian H_0 ($\langle \dots \rangle_0 = \text{Tr}[\exp(-\beta H_0) \dots] / Z_0$) as

$$\Omega = \Omega_0 - \frac{1}{\beta} \ln \langle \hat{S} \rangle_0. \quad (6)$$

Ω_0 is the grand-canonical potential corresponding to H_0 ,

$$\Omega_0 = -\frac{1}{\beta} \ln Z_0, \quad (7)$$

where

$$Z_0 = \text{Tr} \exp(-\beta H_0) = \prod_i Z_0^i \quad (8)$$

is the unperturbed partition function which factorizes into independent single-site partition functions Z_0^i . $\beta = 1/T$ stands for the inverse temperature, and the operator \hat{S} is given by

$$\hat{S} = \mathcal{T} \exp \left[- \int_0^{\beta} d\tau \hat{H}_1(\tau) \right], \quad (9)$$

where \mathcal{T} is the τ -ordering operator, and the interaction Hamiltonian $\hat{H}_1(\tau)$ is in the interaction representation. The LCE theory can now be obtained by expanding the exponential in (9), so that the n th order contribution to $\langle \hat{S} \rangle_0$ is

$$\frac{(-1)^n}{n!} \sum_{11'\sigma_1} \sum_{22'\sigma_2} \cdots \sum_{nn'\sigma_n} t_{11'} t_{22'} \cdots t_{nn'} \int_0^{\beta} d\tau_1 d\tau_2 \cdots d\tau_n$$

$$\langle \mathcal{T} [\hat{c}_{1\sigma_1}^{\dagger}(\tau_1) \hat{c}_{1'\sigma_1}(\tau_1) \hat{c}_{2\sigma_2}^{\dagger}(\tau_2) \hat{c}_{2'\sigma_2}(\tau_2) \cdots \hat{c}_{n\sigma_n}^{\dagger}(\tau_n) \hat{c}_{n'\sigma_n}(\tau_n)] \rangle_0, \quad (10)$$

and expressing the unperturbed ensemble averages in terms of cumulants. Metzner⁹ has proposed a method to calculate the atomic cumulants based on functional differentiation of a generating functional with respect to auxiliary Grassmann fields. In Sec. IV we will introduce another, more convenient, way. Here, we denote the atomic cumulants by M_k^0 and represent them diagrammatically by open circles ($2k$ -valent vertices) with k entering and k leaving lines. A hopping matrix element t_{ij} (or its Fourier transform) will be represented by a directed line (bond). More details about this diagrammatic technique are given in Ref. 9.

The explicit evaluation of Ω can now be performed in terms of diagrams. Due to the use of the cumulant representation, the linked cluster theorem applies in the usual way, so that the first few terms (to the fourth order in t) of the series are

$$-\beta\Omega/N = \circ + \text{loop} + \text{square} + \text{two-loops} + \text{triple-loop} + \dots \quad (11)$$

The zero-valent vertex here represents the zero-order atomic cumulant $M_0^0 = \ln Z_0^i$. Diagram of the form of a triangle does not appear in Eq. (11), because of the choice of the lattices to be hypercubic. For such lattices, diagrams which contain n -gons with odd n do not contribute, since their embeddings vanish. It is convenient to construct the diagrammatic technique in the frequency Fourier space. Moreover, to avoid unnecessary complication, we temporarily assume translational invariance of the system, so that it is convenient to use also momentum representation. Frequencies, spins, and momenta are conserved at vertices. Then, the algebraic expression corresponding to Eq. (11) is

$$\begin{aligned} -\beta\Omega/N = & M_0^0 - \frac{1}{2}\beta^2 \sum_{r_1} [M_1^0(r_1; r_1)]^2 \frac{1}{N} \sum_{\mathbf{q}} (t_{\mathbf{q}})^2 - \frac{1}{4}\beta^4 \sum_{r_1} [M_1^0(r_1; r_1)]^4 \frac{1}{N} \sum_{\mathbf{q}} (t_{\mathbf{q}})^4 \\ & + \frac{1}{2}\beta^4 \sum_{r_1 r_2} M_1^0(r_1; r_1) M_1^0(r_2; r_2) M_2^0(r_1, r_2; r_1, r_2) \left(\frac{1}{N} \sum_{\mathbf{q}} (t_{\mathbf{q}})^2 \right)^2 \\ & + \frac{1}{8}\beta^4 \sum_{r_1 r_2 r_3} M_2^0(r_1, r_3; r_2, r_1 + r_3 - r_2) M_2^0(r_2, r_1 + r_3 - r_2; r_1, r_3) \\ & \times \frac{1}{N^3} \sum_{\mathbf{k} \mathbf{q} \mathbf{p}} t_{\mathbf{k}} t_{\mathbf{q}} t_{\mathbf{p}} t_{\mathbf{k}+\mathbf{q}-\mathbf{p}} + \dots, \end{aligned} \quad (12)$$

where r_i include both spin and frequency variables. $t_{\mathbf{q}}$ is the Fourier transform of the hopping matrix element t_{ij} , and the numerical factors which appear in Eq. (12) are the symmetry factors of the corresponding diagrams.

The idea of the VR is to absorb all possible local insertions at a bare vertex into a renormalized one, i.e., to perform a partial resummation of diagrams. Then, the LCE series can be written in terms of renormalized cumulants, and all the local insertions are removed (the renormalized LCE).^{9,10} To classify various types of insertions according to the clipped bond ends, one has to define the k -particle self-fields G_k as the sum of all topologically distinct local insertions with $2k$ clipped bonds. For example,

$$G_1 \equiv \text{loop} \textcircled{1} = \text{loop} + \text{square} + \text{two-loops} + \dots, \quad (13)$$

$$G_2 \equiv \text{triple-loop} \textcircled{2} = \text{triple-loop} + \dots. \quad (14)$$

Quantities G_k play a physical role of generalized effective fields. The renormalized vertices, which we denote by solid circles, can now be obtained by decorating bare vertices with the self-fields in all possible ways,

$$\bullet = \circ + \text{loop} \textcircled{1} + \text{square} \textcircled{1} + \text{triple-loop} \textcircled{2} + \dots. \quad (15)$$

They represent renormalized cumulants M_k , i.e., cumulants of the partition function Z corresponding to the total Hamiltonian (1) of the system. The renormalization procedure can be applied to vertices in the diagrammatic equations for the self-fields [Eqs. (13) and (14)]:

$$G_1 = \text{loop} \bullet + \text{square} \bullet + \dots, \quad (16)$$

$$G_2 = \text{triple-loop} \bullet + \dots. \quad (17)$$

Hence, the self-fields G_k can be expressed in terms of the renormalized cumulants M_p as sums of appropriate renormalized skeleton diagrams. Then, Eq. (15) becomes a nonlinear equation which can in principle be solved to express M_n in terms of the bare atomic cumulants M_k^0 .

Since diagrams for the grand-canonical potential [Eq. (11)] are unrooted, they have no unique skeletons. Therefore, direct renormalization of vertices in unrooted diagrams is inapplicable and would amount to an overcounting. One has to "count" and subtract

the overcounting,²⁴ or circumvent this obstacle by using other topological²⁵ or algebraic^{9,10} methods. The result is

$$-\beta\Omega/N = M_0 + \Phi - \sum_{r_1} M_1(r_1; r_1) G_1(r_1; r_1) - \sum_{r_1 r_2 r_3} M_2(r_1, r_3; r_2, r_1 + r_3 - r_2) \times G_2(r_2, r_1 + r_3 - r_2; r_1, r_3) - \dots, \quad (18)$$

where Φ is the sum of topologically distinct irreducible (i.e., without local insertions) unrooted vertex-renormalized diagrams, except the single vertex:

$$\Phi = \text{[diagram 1]} + \text{[diagram 2]} + \text{[diagram 3]} + \dots \quad (19)$$

Thus, taking into account the overcounting introduces two effects: renormalization of the zero-order atomic cumulant M_0^0 , and a counter term of the form $-\sum_{n=1}^{\infty} M_n G_n$ called compensating series. Natural variables of the quantity Φ are renormalized cumulants. It is easy to verify by functionally differentiating $\Phi\{M\}$ the useful identity^{9,10}

$$G_n = \frac{\delta\Phi}{\delta M_n}. \quad (20)$$

Despite the VR, the series expansions still involve an infinite number of terms and in practice, at least for the general case, one has to resort to approximate solutions. A general procedure to construct self-consistent approximations is suggested by the above derivation. One has to choose an approximate $\Phi\{M\}$ consisting of a (finite or infinite) subset of terms of Eq. (19). It can be used to find $G_n\{M_k\}$ by Eq. (20). This approximation is then set to Eq. (15) and the resulting equations are solved for M_n , what finally makes Φ and G_n explicit and allows one to calculate the grand-canonical potential according to Eq. (18). Approximations which can be formulated within the frames of the above scheme are called Φ derivable.¹⁰

III. LIMIT OF HIGH LATTICE DIMENSION

To obtain nontrivial infinite-dimensional models, the parameters of the parts of the Hamiltonian which involve intersite couplings must be properly scaled to compensate for the increase in the number of neighbors on the lattice in high dimensions. The nearest-neighbor hopping amplitude t in the Hubbard model (1) must be scaled as

$$t = t^*/\sqrt{z} \quad (21)$$

with fixed t^* . z is the coordination number of the lattice, and for the considered hypercubic lattices $z = 2d$. This scaling is necessary to keep the kinetic energy finite when $d \rightarrow \infty$.²

The Fourier transform of the hopping matrix element is

$$t_{\mathbf{q}} = -2t \sum_{j=1}^d \cos q_j, \quad (22)$$

where $\mathbf{q} = (q_1, \dots, q_d)$, and application of the central-limit theorem leads to the Gaussian density of states of the noninteracting system in the limit of infinite dimension,^{2,3}

$$\rho(\epsilon) \stackrel{d \rightarrow \infty}{=} \frac{1}{t^*} \frac{1}{\sqrt{2\pi}} \exp\left[-\frac{1}{2} \left(\frac{\epsilon}{t^*}\right)^2\right]. \quad (23)$$

Hence, summation over a single momentum variable in this limit reduces to the calculation of a Gaussian integral of the form

$$\frac{1}{N} \sum_{\mathbf{q}} f(t_{\mathbf{q}}) \stackrel{d \rightarrow \infty}{=} \frac{1}{\sqrt{2\pi}} \int_{-\infty}^{\infty} d\epsilon \exp(-\epsilon^2/2) f(\epsilon t^*). \quad (24)$$

The contributions to the grand-canonical potential obtained from the unrenormalized LCE [Eq. (11)] can be classified by powers of the inverse dimension $1/d$ (or $1/z$). The evaluation of diagrams involves lattice sums which amount to counting the number of possible embeddings of the diagram on the lattice. Within the LCE, the summations over lattice sites are *unrestricted* (the so-called “free embedding” or “free multiplicity”⁸). Therefore, it is quite permissible for graphically distinct vertices to occupy the same lattice site. In general, calculation of the free multiplicity lattice constants is rather difficult,³² but for the considered case of high lattice dimension, the problem simplifies considerably.

As an example, let us consider the d dependence of the contributions of the diagrams explicitly shown in Eq. (11). Transforming back to the real space the momentum sum in the second term on the right-hand side of Eq. (12) (this term corresponds to the single-bubble diagram), we get

$$\frac{1}{N} \sum_{\mathbf{q}} (t_{\mathbf{q}})^2 = z t^2. \quad (25)$$

However, due to the scaling (21), each $t \propto 1/\sqrt{z}$, so that the single-bubble diagram in Eq. (11) is $\propto (1/z)^0$ and will survive in the infinite dimensional limit. The square diagram in Eq. (11) has the free-multiplicity lattice constant $3z(z-1)$, and together with the factor t^4 introduced by the four bonds, also provides a nonvanishing contribution in the limit $d \rightarrow \infty$. The same applies to the diagram of the form of two bubbles, as its contribution is $\propto z^2 t^4$. The only diagram among the fourth-order ones which does not contribute to the considered limit is the last diagram in Eq. (11). It carries the factor $z t^4 \propto 1/z$, and vanishes as $d \rightarrow \infty$.

In general, it can be shown^{9,16} that the leading term in z of the free-multiplicity lattice constant of an arbitrary p -gon (with even p) is $\propto z^{p/2}$, and since each line corresponds to $t = t^*/\sqrt{z}$, all such diagrams (of the form of single-loop) survive when $d \rightarrow \infty$. Next, it is easy to convince oneself that adding loops (arbitrary p -gons) to any vertex of a diagram does not change its d depen-

dence (the double-bubble diagram discussed above is an example). Moreover, all the diagrams which are not of the form of loops decorated by other loops are suppressed by some power of $1/d$ as $d \rightarrow \infty$. Therefore, the general conclusion, derived already by Metzner,⁹ is that in the limit of high lattice dimension only diagrams of the form of loops self-consistently decorated by loops contribute.

The key point of our analysis, however, is to notice that all such diagrams are generated by the VR. If we follow the general prescription to construct Φ -derivable approximations described in the preceding section, with Φ chosen to contain all possible vertex-renormalized single-loop diagrams, the self-consistent VR implied by the use of Eqs. (20) and (15) generate all the required diagrams which contribute in the limit $d \rightarrow \infty$. Therefore, the *exact* expression for the functional Φ in this limit is

$$\begin{aligned} \Phi\{M\} &= \text{diagram 1} + \text{diagram 2} + \text{diagram 3} + \dots \\ &= -\frac{1}{2} \sum_{k=1}^{\infty} \frac{1}{k} \beta^{2k} \sum_{\sigma n} [M_1(\sigma, \omega_n)]^{2k} \frac{1}{N} \sum_{\mathbf{q}} (t_{\mathbf{q}})^{2k} \\ &= \frac{1}{2N} \sum_{\mathbf{q}} \sum_{\sigma n} \ln\{1 - [\beta t_{\mathbf{q}} M_1(\sigma, \omega_n)]^2\}, \end{aligned} \quad (26)$$

where $M_1(\sigma, \omega_n) \equiv M_1(\sigma, \omega_n; \sigma, \omega_n)$ is the first-order renormalized cumulant. Note that this is the only cu-

mulant involved. Therefore, as follows from Eq. (20), the only nonzero self-field corresponding to the functional Φ is the single-particle one

$$\begin{aligned} G_1(\sigma, \omega_n) &\equiv G_1(\sigma, \omega_n; \sigma, \omega_n) \\ &= \frac{\delta \Phi}{\delta M_1(\sigma, \omega_n)} \\ &= -\beta^2 M_1(\sigma, \omega_n) \frac{1}{N} \sum_{\mathbf{q}} \frac{(t_{\mathbf{q}})^2}{1 - [\beta t_{\mathbf{q}} M_1(\sigma, \omega_n)]^2}. \end{aligned} \quad (27)$$

Diagrammatically, G_1 is just the sum of all loops, with vertices which in turn themselves can be decorated by loops,

$$G_1(\sigma, \omega_n) = \text{diagram 1} + \text{diagram 2} + \text{diagram 3} + \dots \quad (28)$$

According to Eq. (15), the renormalized vertices which appear in Eq. (26) are the bare ones decorated in all possible ways with this G_1 , so that Φ includes all the diagrams of order $(1/z)^0$, and becomes exact in the limit $d \rightarrow \infty$.

Since G_k vanish for any $k > 1$, renormalization series (15) for the case of the first-order renormalized cumulant takes the algebraic form

$$\begin{aligned} M_1(\sigma, \omega_n) &= M_1^0(\sigma, \omega_n) + \sum_{\tau p} G_1(\tau, \omega_p) M_2^0(\sigma, \omega_n; \tau, \omega_p) \\ &\quad + \frac{1}{2} \sum_{\tau p} \sum_{\varsigma q} G_1(\tau, \omega_p) G_1(\varsigma, \omega_q) M_3^0(\sigma, \omega_n; \tau, \omega_p; \varsigma, \omega_q) + \dots, \end{aligned} \quad (29)$$

where, due to the diagonal (in the frequency and spin variables) form of G_1 , we have used a simplified notation taking $M_k^0(r_1; \dots; r_k) \equiv M_k^0(r_1, \dots, r_k; r_1, \dots, r_k)$. Equation (29) together with Eq. (27) yield the self-consistent equation which is to be solved with respect to M_1 . Finally, we can evaluate the grand-canonical potential according to Eq. (18), which in our case simplifies to

$$-\beta\Omega/N = M_0 + \Phi - \sum_{\sigma n} M_1(\sigma, \omega_n) G_1(\sigma, \omega_n). \quad (30)$$

M_0 here is the zero-order renormalized cumulant which can be obtained by summation of the renormalization series

$$M_0 = M_0^0 + \sum_{\sigma n} G_1(\sigma, \omega_n) M_1^0(\sigma, \omega_n) + \frac{1}{2} \sum_{\sigma n} \sum_{\tau p} G_1(\sigma, \omega_n) G_1(\tau, \omega_p) M_2^0(\sigma, \omega_n; \tau, \omega_p) + \dots \quad (31)$$

We emphasize that Eqs. (26)–(31) are exact in the limit of infinite dimension. However, to be able to sum up the renormalization series (29) and (31), in practical calculation we have to resort to an approximate procedure described in the next section.

IV. DIAGRAMMATIC TECHNIQUE FOR HUBBARD OPERATORS AND SUMMATION OF THE RENORMALIZATION SERIES

The first problem one has to face trying to sum up the renormalization series is that it is necessary to have

a simple and convenient expression for the bare atomic cumulants M_k^0 for arbitrary k . However, the corresponding calculation turns out to be extremely tedious, and the explicit expressions grow enormously with k . On the other hand, the atomic cumulants can also be calculated diagrammatically in terms of a diagrammatic technique for the Hubbard operators (HO). The diagrammatic representation of the terms contributing to M_k^0 becomes particularly convenient in approximate calculation, in which one can perform selective summations of classes of diagrams. Here we use the technique developed by Yang and Wang²² and subsequently extended to the case of

pseudofermion HO by Bartkowiak.²³

The basis of the single-site (atomic) Hilbert subspace is chosen as $|\mathbf{i}e\rangle$ (empty site \mathbf{i} — the vacuum state), $|\mathbf{i}+\rangle \equiv c_{\mathbf{i}+}^\dagger |\mathbf{i}e\rangle$, $|\mathbf{i}-\rangle \equiv c_{\mathbf{i}-}^\dagger |\mathbf{i}e\rangle$, and $|\mathbf{i}d\rangle \equiv c_{\mathbf{i}+}^\dagger c_{\mathbf{i}-}^\dagger |\mathbf{i}e\rangle$, with the corresponding eigenenergies

$$\varepsilon_e^{\mathbf{i}} = 0, \quad \varepsilon_\sigma^{\mathbf{i}} = -\sigma h_{\mathbf{i}} - \mu, \quad \varepsilon_d^{\mathbf{i}} = -2\mu + U. \quad (32)$$

We define 16 HO as

$$L_{\alpha\gamma}^{\mathbf{i}} \equiv |\mathbf{i}\alpha\rangle \langle \mathbf{i}\gamma|, \quad (33)$$

where $\alpha, \gamma = e, +, -, d$. The fermion creation and annihilation operators can be written as linear combinations of HO as

$$c_{\mathbf{i}+}^\dagger = L_{+e}^{\mathbf{i}} + L_{d-}^{\mathbf{i}}, \quad c_{\mathbf{i}-}^\dagger = L_{-e}^{\mathbf{i}} - L_{d+}^{\mathbf{i}}. \quad (34)$$

It follows from Eq. (33) that the commutation relations for the HO are

$$[L_{\alpha\gamma}^{\mathbf{i}}, L_{\kappa\lambda}^{\mathbf{j}}]_\eta = \delta_{\mathbf{i}\mathbf{j}} (\delta_{\gamma\kappa} L_{\alpha\lambda}^{\mathbf{i}} + \eta \delta_{\alpha\lambda} L_{\kappa\gamma}^{\mathbf{i}}), \quad (35)$$

where $\eta = \pm$. The plus sign is used if both operators have pseudofermion character, and the minus sign if at least one of them has pseudoboson character. A Hubbard operator $L_{\alpha\gamma}^{\mathbf{i}}$ is a pseudofermion operator $[(\alpha\gamma) \in \Upsilon_f]$, when the difference between the number of fermions on site \mathbf{i} in state $|\mathbf{i}\alpha\rangle$ and in state $|\mathbf{i}\gamma\rangle$ is odd, and it is a pseudoboson operator $[(\alpha\gamma) \in \Upsilon_b]$, when this difference is even.²⁰ In our case $\Upsilon_f = \{(e\sigma), (\sigma e), (d\sigma), (\sigma d)\}$, and $\Upsilon_b = \{(\sigma\bar{\sigma}), (de), (ed), (ee), (dd), (\sigma\sigma)\}$, where $\sigma = \pm 1$. Moreover, the diagonal HO $L_{\alpha\alpha}$ satisfy the normalization condition

$$\sum_{\alpha} L_{\alpha\alpha}^{\mathbf{i}} = 1. \quad (36)$$

Expressions (34) for fermion operators can be substituted into the expression (10) for the n th-order contribution to $\langle \hat{S} \rangle_0$, so that the LCE can be formulated in terms of HO. The fact that (anti)commutators of HO are linear in HO enables us to prove the Wick theorem and then, with the following procedure, to construct a diagrammatic technique. Each Hubbard orbital produces a HO vertex and vertices are embraced together by ovals in all possible ways, which define single-site blocks. Their appearance follows from the cumulant representation of the unperturbed ensemble averages. Sums of certain single-site blocks correspond to bare vertices in the diagrammatic technique used in the previous sections, and represent atomic cumulants M_k^0 . The dynamics of the system implies appearance of the single-site Green's functions, which are represented diagrammatically in the frequency space as

$$\overrightarrow{\alpha\gamma} \equiv g_{\alpha\gamma}^{\mathbf{i}}(\omega_n) = -\frac{1}{\beta} \frac{1}{i\omega_n - (\varepsilon_{\alpha}^{\mathbf{i}} - \varepsilon_{\gamma}^{\mathbf{i}})}. \quad (37)$$

Here, because of the ‘‘priority rule’’ in using the Wick theorem, $(\alpha\gamma)$ can be any of the following pairs: $(+e), (-e), (de), (-+), (d+)$, and $(d-)$. Depending on the corresponding HO, the Matsubara frequency ω_n is either a boson or a fermion one. Single-site Green's-function lines (37) can appear in many different combinations in single-site blocks. Details of this diagrammatic technique were reported earlier,²³ together with the complete list of HO vertices and their weight factors for the Hubbard model.

In order to obtain a convenient diagrammatic expression for the atomic cumulants, we define the generating functional¹⁹

$$W\{x\} \equiv \exp(y_e + x_{+e} + x_{-e}) + \exp(y_+ + x_{+e} + x_{d+}) \\ + \exp(y_- + x_{-e} + x_{d-}) \\ + \exp(y_d + x_{d+} + x_{d-}), \quad (38)$$

where

$$y_{\alpha} \equiv -\beta \varepsilon_{\alpha}. \quad (39)$$

The site indices in Eqs. (38) and (39) have been dropped, due to the temporarily assumed translational invariance of the system. According to the general graphical rules of the diagrammatic technique for HO,^{22,23} contributions of blocks can be evaluated by taking derivatives of $\ln W$ with respect to appropriate $x_{\alpha\gamma}$ at $x = 0$. If we now change the variables to

$$h_{\sigma} = x_{\sigma e} - x_{d\bar{\sigma}}, \quad (40)$$

the zero-order atomic cumulant takes the form

$$M_0^0 = \ln W = x_{d+} + x_{d-} + \ln(e^{y_e+h_++h_-} + e^{y_++h_+} \\ + e^{y_-+h_-} + e^{y_d}). \quad (41)$$

Due to this, the first-order atomic cumulant

$$M_1^0(\sigma, \omega_n) = \overbrace{\sigma e} + \overbrace{d\bar{\sigma}} \\ = g_{\sigma e}(\omega_n) S_{\sigma e} + g_{d\bar{\sigma}}(\omega_n) S_{d\bar{\sigma}}, \quad (42)$$

where

$$S_{\sigma e} = \frac{e^{y_e+h_++h_-} + e^{y_{\sigma}+h_{\sigma}}}{e^{y_e+h_++h_-} + e^{y_++h_+} + e^{y_-+h_-} + e^{y_d}}, \quad (43)$$

$$S_{d\bar{\sigma}} = 1 - S_{\sigma e},$$

becomes a functional of the variables h_{\pm} only. Therefore, all higher-order cumulants can be expressed in terms of derivatives of $M_1^0(\sigma, \omega_n)$ with respect to h_{τ} . For example,

$$\begin{aligned}
M_2^0(\sigma, \omega_n; \sigma, \omega_p) &= \overline{\sigma e \leftarrow \sigma e} + \overline{\sigma e \leftarrow d\bar{\sigma}} \\
&+ \overline{d\bar{\sigma} \leftarrow \sigma e} + \overline{d\bar{\sigma} \leftarrow d\bar{\sigma}} \\
&= g_{\sigma e}(\omega_p) \left(g_{\sigma e}(\omega_n) \frac{\delta^2 \ln W}{\delta x_{\sigma e}^2} + g_{d\bar{\sigma}}(\omega_n) \frac{\delta^2 \ln W}{\delta x_{\sigma e} \delta x_{d\bar{\sigma}}} \right) \\
&+ g_{d\bar{\sigma}}(\omega_p) \left(g_{\sigma e}(\omega_n) \frac{\delta^2 \ln W}{\delta x_{d\bar{\sigma}} \delta x_{\sigma e}} + g_{d\bar{\sigma}}(\omega_n) \frac{\delta^2 \ln W}{\delta x_{d\bar{\sigma}}^2} \right) \\
&= g_{\sigma}(\omega_p) \frac{\delta M_1^0(\sigma, \omega_n)}{\delta h_{\sigma}}, \tag{44}
\end{aligned}$$

where

$$g_{\sigma}(\omega_p) \equiv g_{\sigma e}(\omega_p) - g_{d\bar{\sigma}}(\omega_p). \tag{45}$$

Diagrams which appear in Eq. (44) contain only simple creation and annihilation HO vertices.²² However, even in the diagrammatic expression for the second-order cumulant for different spin variables,

$$\begin{aligned}
M_2^0(\sigma, \omega_n; \bar{\sigma}, \omega_p) &= \overline{\sigma e \leftarrow \bar{\sigma} e} + \overline{\sigma e \leftarrow d\sigma} \\
&+ \overline{d\bar{\sigma} \leftarrow \bar{\sigma} e} + \overline{d\bar{\sigma} \leftarrow d\sigma} \\
&+ \sum \left(\text{diagram with } \alpha\gamma, \zeta\eta, \alpha\gamma \text{ vertices} \right) + \sum \left(\text{diagram with } \zeta\eta, \kappa\lambda, \alpha\gamma \text{ vertices} \right) \\
&+ \sum \left(\text{diagram with } \zeta\eta, \kappa\lambda, \alpha\gamma \text{ vertices} \right), \tag{46}
\end{aligned}$$

besides terms of the form similar to those in Eq. (44), other terms which involve more complicated (scattering) HO vertices already appear. The symbol \sum in Eq. (46) stands for the sum of diagrams of the following form, with $(\alpha\gamma), (\zeta\eta) \in \Upsilon_f$, and $(\kappa\lambda) \in \Upsilon_b$. Inclusion of the terms which involve scattering HO vertices makes it practically impossible to sum up the renormalization series. Consequently, we assume a serious simplification by keeping only diagrams of the form

$$\overline{\alpha\gamma \leftarrow \kappa\lambda \leftarrow \zeta\eta \leftarrow \dots}, \tag{47}$$

where the Green's-function lines are fermion ones. In fact, this class of diagrams is the only one which appears for the case of cumulants with equal spin variables [as illustrated by Eq. (44)], so that keeping only diagrams of the form (47) remains exact for the case of the Falicov-Kimball model, where only one of the two spin species is allowed to hop. We have checked that the proposed approach allows one to reproduce the exact solution by Brandt and Mielsch⁶ of this model in the limit $d \rightarrow \infty$ (we plan to describe this in detail in a separate publication). For the half-filled-band case discussed in this paper, the above approximation does not violate any general thermodynamic identities and maintains the Φ -derivable character of the proposed approach. The approximation neglects quantum fluctuations between single-site states which involve the interplay of spin-up and spin-down electrons. The quantum fluctuations are important at low temperatures, and the interplay between spin-up and spin-down electrons is important only for small (but finite) U . Therefore, one can

expect that this approximation will not affect seriously the results of the present work, except for the small- U region at low temperatures.

The n th-order cumulants can now be expressed in the general analytical form

$$\begin{aligned}
M_n^0(\sigma_n, \omega_n; \dots; \sigma_1, \omega_1) &= g_{\sigma_1}(\omega_1) \cdots g_{\sigma_{n-1}}(\omega_{n-1}) \\
&\times \frac{\delta^{n-1} M_1^0(\sigma_n, \omega_n)}{\delta h_{\sigma_1} \cdots \delta h_{\sigma_{n-1}}}. \tag{48}
\end{aligned}$$

With such simplification, we can sum up renormalization series (29) for the first-order renormalized cumulant. The final result can be written in the functional form as

$$M_1(\sigma, \omega_n) = M_1^0(\sigma, \omega_n) \{h_+ + \theta_+, h_- + \theta_-\}, \tag{49}$$

where

$$\theta_{\tau} \equiv \sum_p G_1(\tau, \omega_p) g_{\tau}(\omega_p). \tag{50}$$

For calculating the physical quantities of our interest, we set $h_{\pm} = 0$ and, taking into account Eq. (27), arrive at the self-consistent equations for the quantities θ_{σ} ,

$$\begin{aligned}
\theta_{\sigma} &= -\beta^2 \sum_n M_1(\sigma, \omega_n) g_{\sigma}(\omega_n) \frac{1}{N} \\
&\times \sum_{\mathbf{q}} \frac{(t_{\mathbf{q}})^2}{1 - [\beta t_{\mathbf{q}} M_1(\sigma, \omega_n)]^2}, \tag{51}
\end{aligned}$$

where, according to Eqs. (49) and (42),

$$M_1(\sigma, \omega_n) = g_{\sigma}(\omega_n) S_{\sigma e} \{ \theta_+, \theta_- \} + g_{d\bar{\sigma}}(\omega_n). \tag{52}$$

$S_{\sigma\epsilon}(\theta_+, \theta_-)$ is given by Eq. (43) with h_τ replaced by θ_τ . It is important to point out that the role of θ_σ in the present theory for the Hubbard model is similar to that of the Weiss fields in the MFA for spin systems.

Once Eq. (51) is solved, the expression for the renormalized first-order cumulant [Eq. (52)] becomes explicit, and hence the functional Φ and the self-field G_1 can be found by Eqs. (26) and (27), respectively. Finally, summation of renormalization series (31) for the zero-order cumulant gives

$$M_0 = M_0^0 \{\theta_+, \theta_-\} + \sum_{\sigma n} G_1(\sigma, \omega_n) g_{d\bar{\sigma}}(\omega_n), \quad (53)$$

where $M_0^0 \{\theta_+, \theta_-\}$ is the zero-order atomic cumulant of Eq. (41) at $h_\tau = \theta_\tau$ and $x_{d\tau} = 0$. This, using Eq. (30) allows one to evaluate explicitly the grand-canonical potential.

Generalization of the above analyses to two-interpenetrating-sublattices systems is straightforward. Generally, besides the equation for the determination of the chemical potential, there will be four coupled self-consistent equations for θ_σ^v , where $v = \pm$ is the sublattice index. The uniform (or staggered) magnetization per site is obtained by taking the derivative of the grand-canonical potential with respect to the external uniform (or staggered) magnetic field h (or h_s).

V. ANTIFERROMAGNETISM FOR THE CASE OF THE HALF-FILLED ENERGY BAND

For the special case of the half-filled energy band ($n = 1$ and $\mu = U/2$) we can prove that the only solutions of the coupled self-consistent equations are those for which $\theta_+^+ = -\theta_+^- = -\theta_-^+ = \theta_-^- \equiv \theta$. Therefore, we arrive at

$$\begin{aligned} \frac{F}{Nt^*} &= U^* - T^* \ln[2e^{-U^*/(2T^*)} + e^{-\vartheta/T^*} + e^{\vartheta/T^*}] + 4T^* \ln \frac{1}{2}(1 + e^{-U^*/(2T^*)}) + C\vartheta \\ &\quad - 2T^* \frac{1}{\sqrt{2\pi}} \int_{-\infty}^{\infty} d\epsilon \exp(-\epsilon^2/2) \sum_{\sigma=\pm 1} \ln \cosh \frac{x_\sigma(\epsilon)}{2T^*}. \end{aligned} \quad (58)$$

Taking the limit $U^* \rightarrow 0$ in Eqs. (54)–(58) leads to the vanishing magnetization m_a , and to the free energy

$$\frac{F}{Nt^*} = -2T^* \frac{1}{\sqrt{2\pi}} \int_{-\infty}^{\infty} d\epsilon \exp(-\epsilon^2/2) \ln 2 \cosh \frac{\epsilon}{2T^*}. \quad (59)$$

These results are just the ones which one should obtain for the free electron gas on the infinite dimensional lattice. Hence, our approach becomes exact at the limit $U = 0$.

At the ground state ($T^* \rightarrow 0$), we obtain the energy

$$\begin{aligned} \frac{E}{Nt^*} &= \frac{U^*}{2} \left\{ 1 - \frac{1}{\sqrt{2\pi}} \int_{-\infty}^{\infty} d\epsilon \exp(-\epsilon^2/2) \right. \\ &\quad \left. \times [1 + 4(\epsilon/U^*)^2]^{1/2} \right\}, \end{aligned} \quad (60)$$

only one equation. After performing the summation over frequencies, and taking the limit $d \rightarrow \infty$ in the sums over momenta according to Eq. (24), the self-consistent equation, in terms of the normalized variables $T^* \equiv T/t^*$, $U^* \equiv U/t^*$, and $\vartheta \equiv \theta T^*$, can be written in the simple form

$$\begin{aligned} 4\vartheta &= -C (U^*)^2 \frac{1}{\sqrt{2\pi}} \int_{-\infty}^{\infty} d\epsilon \exp(-\epsilon^2/2) \frac{\epsilon^2}{\Delta(\epsilon)} \\ &\quad \times \sum_{\sigma=\pm} \frac{\sigma}{x_\sigma(\epsilon)} \tanh \frac{x_\sigma(\epsilon)}{2T^*}, \end{aligned} \quad (54)$$

where

$$C \equiv \frac{e^{\vartheta/T^*} - e^{-\vartheta/T^*}}{2e^{-U^*/(2T^*)} + e^{-\vartheta/T^*} + e^{\vartheta/T^*}}, \quad (55)$$

and

$$\begin{aligned} x_\sigma(\epsilon) &\equiv \frac{1}{2} [(U^*)^2 + 2(\epsilon^2 + \sigma\Delta)]^{1/2}, \\ \Delta &\equiv [\epsilon^2(\epsilon^2 + (U^*)^2(1 - C^2))]^{1/2}. \end{aligned} \quad (56)$$

For the considered case of $n = 1$, the uniform magnetization always vanishes, whereas the antiferromagnetic order parameter (the staggered magnetization per site) can be expressed in terms of the self-consistent solutions of Eq. (54) as

$$m_a = C - 2\vartheta/U^*. \quad (57)$$

Hence, the solution $\vartheta = 0$ corresponds to the paramagnetic phase. The free energy of the system, $F = \Omega + \mu n$, has the general form

with the sublattice magnetization

$$\begin{aligned} m_a &= \frac{1}{\sqrt{2\pi}} \int_{-\infty}^{\infty} d\epsilon \exp(-\epsilon^2/2) [1 + 4(\epsilon/U^*)^2]^{-1/2} \\ &= \frac{U^*}{2\sqrt{2\pi}} \exp[(U^*/4)^2] K_0((U^*/4)^2), \end{aligned} \quad (61)$$

where $K_0(x)$ is the modified Bessel function of the second kind. The antiferromagnetic phase is stable for any U^* , except $U^* = 0$.

The temperature dependence of the order parameter m_a has been computed numerically using Eqs. (54)–(57), and is shown in Fig. 1. For $U^* > 0.3$, m_a decreases monotonically with increasing temperature. But for very small values of U^* , the initial increase of m_a with temperature suggests an inadequacy of the approximation introduced in Sec. IV in the small- U region. The neglected quantum fluctuations between single-site states, described by

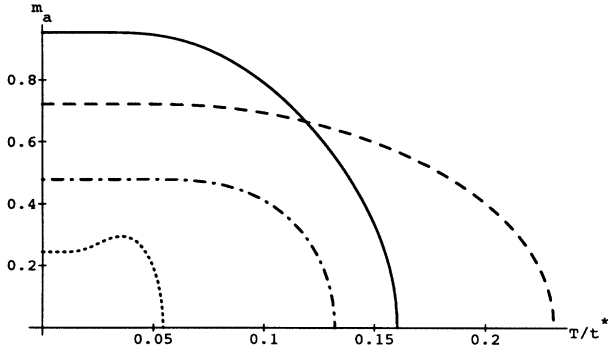


FIG. 1. Sublattice magnetization vs temperature for $U/t^* = 0.2$ (dotted curve), 0.6 (dash-dotted curve), 1.5 (dashed curve), and 6.0 (solid curve).

diagrams containing scattering HO vertices, should suppress this increase of the order parameter. For any value of U^* , it follows from the expansion of the right-hand side of Eq. (57) that near the critical temperature T_N^* , $m_a(T^*) \propto (T_N^* - T^*)^{1/2}$. Hence, the derived sublattice magnetization exhibits the typical mean-field behavior.

The solid curve in Fig. 2 is the Néel temperature obtained by taking the limit $\vartheta \rightarrow 0$ in Eq. (54). The dashed curve, shown in Fig. 2 for comparison, represents the critical temperature calculated from the second-order renormalized LCE,³¹ where the series for the generating functional Φ in Eq. (26), which is exact in the limit $d \rightarrow \infty$, has been truncated at the first (the second order in t) diagram. It is seen that the inclusion of all the higher-order loop diagrams gives lower critical temperature, but the shapes of both curves are very similar. However, it is important to point out that, in contrast to the present calculation, the second-order calculation does not reproduce the exact results for free energy and order parameter at the $U = 0$ limit.³¹ The MFA transition temperature of the effective antiferromagnetic Heisenberg Hamiltonian with $J = 4t^2/U$ is shown in Fig. 2 as the dotted curve. Both the solid and the dashed curves asymptotically approach this result in the large- U limit. Since the MFT for the Heisenberg model is exact in $d = \infty$ dimensions, this agreement indicates that, as expected, the approximation of keeping only diagrams of the form (47), introduces practically no effect in the region of strong correlations. On the other hand, as follows from the small- U perturbation theory³³ and from the numerical study of Jarrell,⁷ T_N should be exponentially small for small values of U , whereas in our result it is almost linear in U [$T_N^* \propto (a - b \ln U^*) U^*$]. This (as has been discussed in the preceding section) is because the introduced approximation leaves out quantum fluctuations between single-site states which involve the interplay of motion of spin-up and spin-down electrons. These fluctuations are responsible for the decrease of the critical temperature. Note that the solid curve in Fig. 2 is very similar in shape to the one obtained by Brandt and Mielsch for the critical

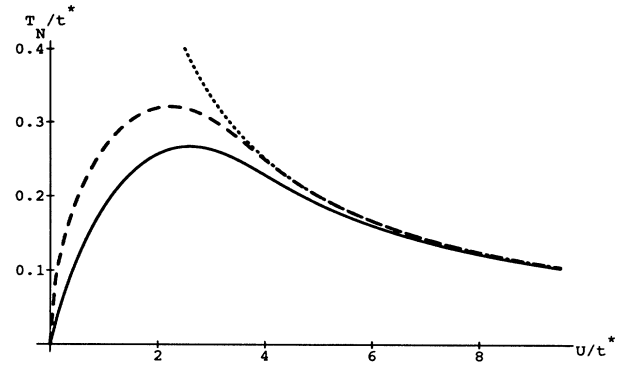


FIG. 2. Néel temperatures computed from the renormalized LCE within the present approach (solid curve), and in the second order (dashed curve). The dotted curve is the MFA result for the effective antiferromagnetic Heisenberg Hamiltonian with $J = 4t^2/U$.

temperature in the exact solution of the Falicov-Kimball model.⁶

VI. CONCLUSIONS

The vertex-renormalized LCE has been used to derive the exact expressions for the generating functional Φ in the limit $d \rightarrow \infty$, the self-fields, and the grand-canonical potential of the Hubbard model. Using the diagrammatic technique for HO, we have then developed an approximate method to sum up the renormalization series for the cumulants. The approximation consists in neglecting diagrams which contain scattering HO vertices in the diagrammatic expressions for the atomic (unrenormalized) cumulants. Such diagrams describe quantum fluctuations between single-site states which involve the interplay of spin-up and spin-down electrons.

Our VR scheme leads to a set of self-consistent equations similar to those in the MFT for spin systems, and consequently to a self-consistent symmetry breaking. Therefore, it provides a basis to study various magnetic orderings of the system at arbitrary temperature. We have presented solutions for the case of the half-filled energy band. The obtained results are exact both in the limit of $U \rightarrow 0$ (free electrons on the infinite dimensional lattice), and in the large- U region, reproducing the exact Heisenberg mean-field behavior in the limit $d \rightarrow \infty$. The proposed approach is valid for the whole range of temperatures and for arbitrary U , except for the region of very small (but finite) U/t^* , where the neglected quantum fluctuations become important.

A possible direction to develop the present scheme is to generate the $1/z$ (or $1/d$) expansion.^{2,9} Within the proposed LCE-based approach, this is relatively simple. Although there are an infinite number of diagrams for Φ which contribute to a certain order in $1/d$, no higher-order VR is necessary, and the corresponding diagram-

matic series are easy to sum up.

The described method is quite general, and, using the diagrammatic technique for HO, can be easily adopted to other strongly correlated fermion systems. In some cases [e.g., the Falicov-Kimball model and the quantum lattice gas model (the so-called "spinless fermion" model)], no approximation is necessary to sum up the renormalization series, and the method can be used to obtain exact solutions in the limit of infinite dimension.³⁴

ACKNOWLEDGMENTS

We are grateful to Professor Yu. A. Izyumov, Professor G. D. Mahan, Professor R. Micnas, Dr. A. Koper, and E. Halvorsen for valuable discussions. Financial support from the Royal Norwegian Council for Scientific and Industrial Research (NTNF) and from the Polish Committee of Scientific Research (KBN) under Grant No. 2 00 68 91 01 is gratefully acknowledged.

*On leave from A. Mickiewicz University, Institute of Physics, PL-60769 Poznań, Poland.

¹J. Hubbard, Proc. R. Soc. London Ser. A **276**, 238 (1963); M.C. Gutzwiller, Phys. Rev. Lett. **10**, 159 (1963); J. Kanamori, Prog. Theor. Phys. **30**, 275 (1963).

²W. Metzner and D. Vollhardt, Phys. Rev. Lett. **62**, 324 (1989).

³E. Müller-Hartmann, Z. Phys. B **74**, 507 (1989); **76**, 211 (1989).

⁴P.G.J. van Dongen and D. Vollhardt, Phys. Rev. Lett. **65**, 1663 (1990); P.G.J. van Dongen, Phys. Rev. B **45**, 2267 (1992).

⁵D. Vollhardt, Int. J. Mod. Phys. B **3**, 2189 (1989); Physica B **169**, 277 (1991); E. Müller-Hartmann, Int. J. Mod. Phys. B **3**, 2169 (1989).

⁶U. Brandt and C. Mielsch, Z. Phys. B **75**, 365 (1989); **79**, 295 (1990).

⁷M. Jarrell (unpublished).

⁸*Phase Transitions and Critical Phenomena*, edited by C. Domb and M.S. Green (Academic, London, 1974), Vol. 3.

⁹W. Metzner, Phys. Rev. B **43**, 8549 (1991).

¹⁰M. Wortis, in *Phase Transitions and Critical Phenomena* (Ref. 8).

¹¹G. Beni, P. Pincus, and D. Hone, Phys. Rev. B **8**, 3389 (1973); M. Plischke, J. Stat. Phys. **11**, 159 (1974); K. Kubo, Prog. Theor. Phys. **64**, 758 (1980); B.-H. Zhao *et al.*, Phys. Rev. B **36**, 2321 (1987).

¹²K.-K. Pan and Y.-L. Wang, Phys. Rev. B **43**, 3706 (1991); M. Bartkowiak and K.A. Chao (unpublished).

¹³K.-K. Pan and Y.-L. Wang, J. Appl. Phys. **69**, 4656 (1991).

¹⁴D.F.B ten Haaf and J.M.J. van Leeuwen (unpublished); J.A. Henderson, J. Oitmaa, and M.C.B. Ashley (unpublished).

¹⁵B. Mühlischlegel and H. Zittartz, Z. Phys. **175**, 553 (1963).

¹⁶R.S. Fishman and G. Vignale, Phys. Rev. B **44**, 658 (1991).

¹⁷B. Westwański and A. Pawlikowski, Phys. Lett. **43A**, 1458 (1973).

¹⁸V.G. Vaks, A.I. Larkin, and S.A. Pikin, Zh. Eksp. Teor. Phys. **53**, 281 (1967) [Sov. Phys. JETP **26**, 188 (1968); **53**, 1089 (1967) **26**, 647 (1968)].

¹⁹Yu.A. Izyumov and Yu.N. Skryabin, *Statistical Mechanics of Magnetically Ordered Systems* (Consultants Bureau, New York, 1989).

²⁰J. Hubbard, Proc. R. Soc. London Ser. A **277**, 237 (1963); **285**, 542 (1965); **296**, 82 (1966); **296**, 100 (1966).

²¹R.O. Zaitsev, Zh. Eksp. Teor. Phys. **70**, 1100 (1976) [Sov. Phys. JETP **43**, 574 (1976)].

²²D.H.-Y. Yang and Y.-L. Wang, Phys. Rev. B **10**, 4714 (1974); **12**, 1057 (1975).

²³M. Bartkowiak, Int. J. Mod. Phys. B **1**, 1277 (1987).

²⁴G. Horwitz and H. Callen, Phys. Rev. **124**, 1757 (1961).

²⁵F. Englert, Phys. Rev. **129**, 567 (1963); C. Bloch and J.S. Langer, J. Math. Phys. **6**, 554 (1965).

²⁶Z. Onyszkiewicz, Phys. Lett. A **76**, 411 (1980).

²⁷Yu.A. Izyumov, F.A. Kassan-Ogly, and Yu.N. Skryabin, J. Phys. (Paris) Colloq. **325**, C1-87 (1971).

²⁸M. Bartkowiak, P. Münger, and R. Micnas, Int. J. Mod. Phys. B **2**, 483 (1988).

²⁹E. Halvorsen and M. Bartkowiak (unpublished).

³⁰M.Yu. Nikolaev, N.V. Ryzhanova, A.V. Vedyayev, and S.M. Zubritskii, Phys. Status Solidi B **128**, 513 (1985).

³¹M. Bartkowiak and K.A. Chao, Phys. Rev. B **47**, 1616 (1993).

³²F. Lee and H.H. Chen, Phys. Rev. B **30**, 2724 (1984); C. Wentworth and Y.-L. Wang, *ibid.* **36**, 8687 (1987).

³³P.G.J. van Dongen, Phys. Rev. Lett. **67**, 757 (1991).

³⁴M. Bartkowiak and E. Halvorsen (unpublished).